Process Systems Engineering

A Novel Approach to Alarm Causality Analysis Using Active Dynamic Transfer Entropy

Yi Luo, Bhushan Gopaluni, Yuan Xu, Liang Cao, and Qun-Xiong Zhu

Ind. Eng. Chem. Res., **Just Accepted Manuscript** • DOI: 10.1021/acs.iecr.9b06262 • Publication Date (Web): 14 Apr 2020

A Novel Approach to Alarm Causality Analysis Using Active Dynamic Transfer Entropy

*Yi Luo[abc], Bhushan Gopaluni[c], Yuan Xu[ab], Liang Cao[c], Qun-Xiong Zhu[ab]**

a.College of Information Science & Technology, Beijing University of Chemical Technology, Beijing, 100029, China;

b. Engineering Research Center of Intelligent PSE, Ministry of Education of China, Beijing 100029, China;

c. Department of Chemical and Biological Engineering, University of British Columbia, Vancouver, BC, Canada;

** Corresponding author: Tel.: +86-10-64413467. Email addresses: buctielab@hotmail.com*

ABSTRACT

Alarm flooding is a serious safety problem in the chemical process industries. Bayesian Networks are a set of powerful tools that can be used to trace the root-cause of alarms. For highly integrated complex chemical processes, we propose a Bayesian Network based on Active Dynamic Transfer Entropy (ADTE) to establish an accurate alarm propagation network during an alarm flood. The proposed method has two primary advantages: (1) it circumvents the false causality problem caused by strong correlations and therefore can be used to mine deeper alarm propagation paths like feedback loops. (2) It provides the time of origin of an alarm as it propagates through the process network, allowing operators to respond appropriately. The proposed method involves the following elements: modular segmentation, extraction of common cause variables, calculation of alarm propagation time between variables, calculation of ADTE, identification of an underlying alarm network and tuning of relevant parameters. The Tennessee Eastman Process (TEP) is used to demonstrate the validity and superiority of the proposed ADTE-based alarm causality method.

Nomenclature

x_i, x_j, x_y, x_o	Continuous random variables
x_{i_p}	Parent variables of x_i
x_{i_c}	Common cause variables of x_i
$T_{x_{i_p} \to x_i}$	Transfer entropy from x_{i_p} to x_i
$T_{(x_{i_p} \to x)^{nor}}$	Normalized transfer entropy from x_{i_p} to x_i
$D_{x_{i_p} \to x_i}$	Direct transfer entropy from x_{i_p} to x_i
$ATE_{x_{i_p} \to x_i}$	Active transfer entropy from x_{i_p} to x_i
$ADTE_{x_{i_p}{}^{t-h} \to x_i}$	Active dynamic transfer entropy from x_{i_p} to x_i with propagation time h

1. INTRODUCTION

Modern industrial plants are highly integrated and extremely complex[1]. As such, it is of utmost importance to operate them safely and efficiently while avoiding catastrophic events that can lead to casualties, significant economic losses and environmental pollution. In the past two decades, the process modeling, process monitoring and control systems, such as Distributed Control System (DCS) and Supervisory Control and Data Acquisition (SCADA), have evolved to incorporate various software tools for this purpose[2,3]. As a result, the performance of industrial alarm systems has improved significantly. However, in practice, alarm flooding problem occurs due to an excessive number of alarms[4-7]. A typical alarm flooding problem includes invalid and repeated alarms, making it difficult for operators to prioritize and separate critical alarms. Alarm flooding problem can be resolved by finding the

root-cause of alarms from many correlated alarms using causality analysis and fault diagnosis methods[8,9].

Causality analysis is a powerful approach often used to trace the root-cause of alarms and establish the causal network of alarms in complex chemical processes. When an alarm flood occurs, causality analysis can be used to provide operators with approximate information about the root-cause and therefore ensure the safety of underlying processes[8,9].

In the research of causal analysis of industrial processes, a causal network of alarms can be built by symbol directed graph (SDG) using a large amount of expert knowledge. These methods have been applied to industrial problems with some success[10,11]. However, in many practical problems, the expert knowledge is limited and therefore it is difficult to establish a causal network that covers all existing relationships between process variables. With the development of the SCADA and the DCS systems, large amounts of data are measured and stored during process operations. These incredible volumes of data facilitate the studies of data-driven methods. There are several effective methods for finding relationships between process variables including interpretable structural models[12,13], Bayesian networks[14-17], Granger causality analysis[18-20] and transfer entropy[20-22]. For Granger causality analysis and transfer entropy, the latter approach is known to provide information about the causal networks especially when the data are limited[23]. However, both of these methods generally exhibit similar performance when there are enough data[20,23]. In a focused study to solve the alarm flood problem, Hu has made noteworthy contributions about the cause-effect between variables by transfer entropy[22,24]. Similar to SDG, the Bayesian Network (BN) based approaches can infer the causality among variables using prior expert knowledge. Moreover,

the Bayesian Network approach is more suitable than SDG for extracting the causal relationships as they provide additional information in the form of probabilistic expressions. Granger causality analysis and transfer entropy are two powerful tools for establishing pairwise causality of variables and therefore have been used in conjunction with Bayesian Networks.

The research on using Bayesian Networks for alarm causality analysis includes two subareas: parameter training and structure learning[24,25]. In parameter training, the underlying structure of the Bayesian network is fixed and the relevant parameters are estimated using data. It is possible to use either raw data or extracted features using Principal Component Analysis (PCA) to train the Bayesian Network parameters[26]. For chemical processes with nonlinear data, a kernel PCA approach[27] is generally used on the raw data before training the parameters of the Bayesian Network. In structure learning, the objective is to construct the structure of Bayesian Network as is done by "scoring and structure" search methods[14]. The basic premise of these scoring algorithms is to quantify the accuracy of a given Bayesian Network using a score. The more accurate the scoring calculation and the more efficient the structure search algorithms are, the better the reconstruction of Bayesian Networks. Two widely used scoring metrics are Bayesian information criterion (BIC)[28] and the Bayesian Dirichlet Equivalence (BDE)[29]. Antoniak[30] proposed a Bayesian Network construction model combining a hybrid search method and the BDE score criterion. By adding a penalty to the complexity of the model using the BIC score, a more simplified model is obtained. However, BIC and BDE criteria are often not good enough to provide acceptable scoring results in complex chemical processes. Hence, the entropy value is used as an alternative scoring

criterion to estimate the Bayesian Network structure in these processes[25]. Meng[31] established a criterion called “family transfer entropy probability” and verified the effectiveness of using transfer entropy based on the score and structure search method.

Methods that rely on causality analysis such as Granger causality, transfer entropy and cross-correlation functions simply provide correlation information and are therefore not reliable in constructing the underlying process structures. The alarm networks are often constructed by these methods focusing on the similarity of the alarm and get false causal results. To this end, Duan proposed the Direct Transfer Entropy (DTE) method[32] to analyze whether the relationship between process variables is direct or indirect. Duan also proposed the Transfer zero-entropy method[32] to analyze the dataset which does not follow a well-defined distribution. In order to further solve the causal propagation of alarms, not just the similarity of alarms. In this paper, we propose a multi-blocks Bayesian Network model based on Active Dynamic Transfer Entropy (ADTE). The industrial process can be divided into several blocks which include several variables in each block. The purpose of multi-blocks segmentation is to adapt to the complexity of chemical data and to ensure accuracy, unlike the traditional Bayesian Networks based on transfer entropy. The ADTE-based multi-blocks Bayesian network model focuses on finding the causality relationship rather than only the alarm similarity relationship, which has important implications in the modeling of alarm systems.

The main contribution of this paper is an algorithm to identify the propagation of alarms through a complex process network using the concepts of Active Dynamic Transfer Entropy and Bayesian Networks. The operators can use the path of alarm propagation to mitigate

alarm flooding. In addition, we propose the concepts of alarm propagation time and alarm propagation structures. With the proposed approach, operators can not only identify the root cause for alarm flooding but also predict the variables to which alarms will spread in future.

This article is organized as follows: the traditional Bayesian Networks, DTE and block segmentation methods for chemical processes will be introduced in Section 2; In Section 3, an approximation of ADTE will be introduced. In addition, the calculation of alarm propagation time and the construction of alarm propagation structure with time information will be introduced in detail. In Section 4, the TEP benchmark is used to illustrate the advantages of the proposed method. Conclusions are presented in Section 5.

2. PRELIMINARIES

In this section, the traditional Bayesian Network will be introduced and the BDE, BIC and TE criteria for scoring a structure will be briefly compared. In addition, this section will also introduce the basic DTE methods and the block segmentation method for chemical processes. These methods are then used in developing the ADTE-based multi-blocks Bayesian Network.

2.1 Bayesian Network

A Bayesian Network shows the relationship between different process variables and the strength of those relationships by using graph models and probability. Bayesian Networks are widely used in chemical processes. Several data-driven methods can be used to construct a Bayesian Network among which the score and structure search approach is better than other methods[34].

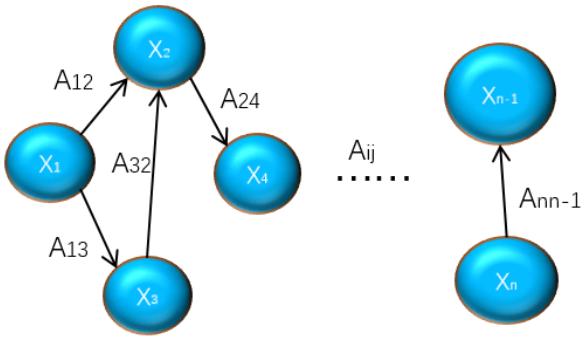

Fig.1 The structure of Bayesian Network

Let us consider a process structure with variables x_1 to x_n connected as shown in Figure.1. The measurement of a variable x_i at time $t=l$ is denoted by x_i^l. Given measurements of the n variables from time $t=1$ to $t=m$, we define the data matrix $X \in R^{m\times n}$ as follows:

$$X=\begin{bmatrix} x_1^t & x_2^t & \dots & x_n^t \\ x_1^{t+1} & x_2^{t+1} & \dots & x_n^{t+1} \\ \dots & \dots & \dots & \dots \\ x_1^{t+m-1} & x_2^{t+m-1} & \dots & x_n^{t+m-1} \end{bmatrix}$$

If a connection exists from x_1 to x_2, then x_1 is referred as parent variable, and x_2 is referred as child variable, and the transfer correlation is from x_1 to x_2. All the parent variables of x_i are represented by x_{i_p}.

In addition, we also define an adjacent matrix A with elements a_{ij},

$$A=\begin{bmatrix} a_{11} & a_{12} & \dots & a_{1n} \\ a_{21} & a_{22} & \dots & a_{2n} \\ \dots & \dots & a_{ij} & \dots \\ a_{n1} & a_{n2} & \dots & a_{nn} \end{bmatrix} \in R^{n\times n}$$

where i refers to the i^{th} variable x_i and j refers to the j^{th} variable x_j. If a direct connection exists between x_i and x_j then $a_{ij}=1$ otherwise $a_{ij}=0$. The matrix A simply provides information about the existence of connections between different variables. Using a new matrix Θ we capture the strength of these connections, which can be

measured using a variety of metrics such as BIC, BDE, and TE, etc.

$$\Theta = \begin{bmatrix} \theta_{11} & \theta_{12} & \ldots & \theta_{1n} \\ \theta_{21} & \theta_{22} & \ldots & \theta_{2n} \\ \ldots & \ldots & \theta_{ij} & \ldots \\ \theta_{n1} & \theta_{n2} & \ldots & \theta_{nn} \end{bmatrix} \in R^{+^{n\times n}}$$

With the above definitions, any given process structure can be characterized by the tuple $G = \langle X, A, \Theta \rangle$ where G represents the corresponding structure and the relevant information. Given a set of structures $G^{all} = \{G_1 \quad G_2 \quad \ldots \quad G_T\}$, for every structure G_s, we define a score which is calculated by one of the scoring functions in Equations. 2, 3 or 5. The class of Score and Search (SS) methods are based on the data matrix X and score for each structure $G_s \in G^{all}$. These methods choose the structure $G_{\max}$ with the highest score as the optimal structure. The evaluation criterion is shown as follows,

$$G_{\max} = \arg\max_{G_s \in G^{all}} score(G_s) \qquad (1)$$

where $score(G_s)$ represents the score for structure G_s. The score is determined using criteria such BIC, BDE and TE. BIC and TE focus more on the information flow of Bayesian structure. While the optimal structure obtained by BIC is often relatively simple, TE on the other hand often captures more accurate nonlinear relationships. The score using BIC[28] for structure is defined as follows,

$$BIC(G_s) = \sum_{i=1}^{n}\sum_{j=1}^{q_i}\sum_{k=1}^{r_i}\left(\mathrm{P}_{ijk}\log\left(\frac{\mathrm{P}_{ijk}}{\mathrm{P}_{ij}}\right)\right) - \frac{1}{2}\log(m)\sum_{i=1}^{n}\left((r_i - 1)q_i\right) \qquad (2)$$

where $q_i \in R^+$, and $r_i \in R^+$ represent the number of parent variables and the number of directed edges of each child variable x_i, respectively. n and $\mathrm{P}_{ij} = \sum_{k=1}^{r_i}\mathrm{P}_{ijk}$ represent the number of variables and the probability of different states k of the edge A_{ij}, respectively. P_{ijk} means the probability of the i^{th} variable being in the kth state while the

parent variable is in the j^{th} state.

The TE[25] criterion for evaluation is as follows,

$$TE\left(G_s\right)=\sum_{i=1}^{n}\left(T_{x_{i_p}\to x_i}\text{-}\lambda\log\left(q_i\left(r_i-1\right)\right)\right) \tag{3}$$

where $q_i \in R^+$, and $r_i \in R^+$ represent the number of parent variables and the number of directed edges of each child variable x_i, respectively. λ is a scalar parameter used to penalize the model complexity. And $T_{x_{i_p}\to x_i}$ represents the transfer entropy value of the directions from x_{i_p} to x_i. The TE score is calculated as follows,

$$T_{x_{i_p}\to x}=\sum_{x_i^{t+1},x_i^t,x_{i_p}{}^t} p\left(x_i^{t+1},x_i^t,x_{i_p}{}^t\right)\log_2\frac{p\left(x_i^{t+1}\middle|x_i^t,x_{i_p}{}^t\right)}{p\left(x_i^{t+1}\middle|x_{i_p}{}^t\right)} \tag{4}$$

Since there always exists transfer entropy value between any two variables, a significance test is needed to determine whether a transfer relationship does exist between variables. Therefore, the 95% significance test is used for further screening the effective relationships in this paper, which are described in Yu[21] and Hu's[22] papers. Unlike BIC and TE algorithms based on information flow, BDE[29] calculates the prior probability between variables based on the sampled data, and establishes a model that maximizes the posterior probability of the data, as shown below:

$$BDE(G_s)=\sum_{i=1}^{n}\left[\sum_{j=1}^{q_i}\left[\log\frac{\Gamma\left(\alpha_{ij}\right)}{\Gamma\left(\alpha_{ij}+m_{ij}\right)}+\sum_{k=1}^{r_i}\log\frac{\Gamma\left(\alpha_{ijk}+m_{ijk}\right)}{\Gamma\left(\alpha_{ijk}\right)}\right]\right]+\log\left(d_{G_s}\right) \tag{5}$$

where $\alpha_{ij}=\sum_{k=1}^{r_i}\alpha_{ijk}$ represents the prior probability between variables, and d_{G_s} represents the number of directed edges in the structure G_s. Γ represents the Γ function. Compared with the Bayesian network construction based on expert knowledge, the above three structure construction methods have better performance in practical

applications.

2.2 Direct Transfer Entropy

DTE is an extended version of TE that is used to determine whether the information transfer between variables is direct or indirect. The calculation of TE is shown in Equation.4. The TE is a measure of the prediction accuracy of x_i^{t+1} using $x_{i_p}{}^t$ without the information of x_i^t. A large TE implies that x_{i_p} can predict x_i. However, the TE method cannot determine whether there are other variables exists in the propagation path of x_{i_p} to x_i.

The DTE is calculated as follows[32]:

$$D_{x_{i_p}\to x_i} = \int p\left(x_i^{t+1}, x_i^t, x_j^t, x_{i_p}{}^t\right)\log\frac{p\left(x_i^{t+1}\middle|x_i^t, x_j{}^t, x_{i_p}{}^t\right)}{p\left(x_i^{t+1}\middle|x_i^t, x_j{}^t\right)}dv \qquad (6)$$

where v denotes the random vector$\left[x_i^{t+1}, x_i^t, x_j{}^t, x_{i_p}{}^t\right]$. In the DTE method, we analyze the information of x_i^{t+1} that is obtained from $x_{i_p}{}^t$, but without the information from x_i^t and $x_j{}^t$, where $x_j \in X$ is the middle variable. Similarly, DTE also needs to be tested for significance. If the value of DTE is significant, it indicates that x_{i_p} can directly predict x_i; if the value of DTE is not significant, but the value of TE is significant, it indicates that the information transferring from x_{i_p} to x_i occurs through the variable x_j. This observation helps in further analysis of the relationship between variables in the structure.

2.3 System Blocks Segmentation

Considering that typical chemical plants have many units, we can reduce the workload of building Bayesian structure and improve the accuracy of the structure through block segmentation[21,31]. In the actual chemical process, we can utilize priori process knowledge to divide the chemical process into multiple blocks according to following four steps:

Step 1: The overall chemical process is roughly divided into existing critical process units, such as reactors, condensers etc.

Step 2: According to the expert knowledge of variable correlation and process information such as energy flow or control loop, variables which are not well classified are added to each sub-block;

Step 3: Define the variables connecting adjacent sub-blocks as the associated variables of the two sub-blocks, and these associated variables are used in both adjacent sub-blocks for Bayesian network structure learning;

Step 4: Connect multiple sub-blocks through associated variables between two sub-blocks to restore the structure of the complete chemical process.

3. THE PROPOSED METHODS

Using the definitions from the previous section, we propose an ADTE-based multi-blocks Bayesian network and use this method to construct a Bayesian network structure, which describes the causal relationships between process variables in a real plant. The available causal analysis methods are prone to several challenges such as two variables having high similarity but no real causal relationship. Traditional methods such as Granger causal analysis, Transfer entropy, and Bayesian networks are not effective at separating variables with high similarity from those with causal relationships. To solve this problem, we introduce the ADTE-based multi-blocks Bayesian network in detail below. This method is less prone to false causality relationships but identifies the causal networks with better accuracy. In addition, the obtained alarm propagation paths can be used to identify the source of alarm flooding.

3.1 Identify Common Cause Variables

In the process of constructing a Bayesian network, it is important to identify common cause variables to minimize the risk of falsely assigning causal relationships between variables. As shown in Figure. 2, assuming there are four variables $\{x_i, x_j, x_y, x_o\}$ in chemical process, and two transfer relations $x_i \to x_o$ and $x_i \to x_j$, then there will be higher probability that similar data trends exists between x_i, x_j and x_i, x_o. As a result, the correlation between x_j and x_o is strong. We define x_i as a common cause variable of x_j, x_o. Therefore, we can determine whether there is a common cause variable on the propagation path according to the transfer entropy value. Since the value of the transfer entropy will not be 0 in the actual process, it is necessary to determine whether there is a common cause variable through a significance test by the following criterion,

$$T_{(x_{i_p} \to x)^{nor}} = T_{x_{i_p} \to x} - T_{(x_{i_p} \to x)^r} \tag{7}$$

where $T_{(x_{i_p} \to x)^r}$ represents the threshold of significant test[31,32], $T_{(x_{i_p} \to x)^{nor}}$ represents the normalized transfer entropy value. All variables x_{j_p} that satisfy Equation.8 are considered as common cause variables for the propagation paths from x_j to other variables.

$$T_{(x_{j_p} \to x_j)^{nor}} > 0 \tag{8}$$

where $T_{(x_{j_p} \to x_j)^{nor}}$ represents the transfer entropy value from x_{j_p} to x_j after normalized by Equation.7, if $T_{(x_{j_p} \to x_j)^{nor}} > 0$, it means the transfer relationship from x_{j_p} to x_j is significant, x_j has common cause variables and we should remove them when analyzing the causality from x_j to x_o. The reason for this judgment is that when calculating the active transfer entropy of x_j to x_o, it is necessary to ensure that x_j does not receive information from other variables, and the information received by x_y has no effect on the

active transfer entropy calculation of x_j to x_o.

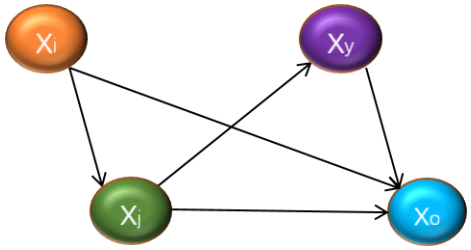

Fig.2 Common cause variable interpretation

where x_i is the parent variable of x_j and x_y is the intermediate variable of x_j and x_o. When calculating the active transfer entropy from x_j to x_o, x_i is regarded as a common cause variable, but there is no need to regard x_y as a common cause variable. If the transfer path is from x_j to x_o, instead of from x_j to x_y and then to x_o. When calculating the path x_y to x_o, x_j is regarded as the parent variable of x_y and also the common cause variable of x_y and x_o, and the path from x_y to x_o will generate a smaller transfer entropy value compared with the path x_j to x_y and then to x_o.

3.2 Active Transfer Entropy

In the alarm system, the data is divided into alarm data and normal data, wherein the alarm data is divided into high alarm data and low alarm data. In this paper, the alarm data of X_i at the sample time t is defined as $A_i^t \in R$, which is generated by the alarm system is discretized as follows:

$$a_i^t = \begin{cases} 1, & x_i^t < A_{i^u} \\ 2, & A_{i^l} < x_i^t < A_{i^u} \\ 3, & x_i^t > A_{i^l} \end{cases} \tag{9}$$

Where $A_{i^l} \in R$ and $A_{i^u} \in R$ represent the low threshold and high threshold of x_i in the process. For discrete data, the discretized ATE can be defined as follows:

$$ATE_{x_{i_p}\to x_i}=\sum_{x_i^{t+1},x_i^t,x_{i_c}^t,x_{i_p}{}^t} p\left(x_i^{t+1},\mathrm{x}_i^t,x_{i_c}^t,x_{i_p}{}^t\right)\log_2\frac{p\left(x_i^{t+1}\middle|x_i^t,x_{i_c}^t,x_{i_p}{}^t\right)}{p\left(x_i^{t+1}\middle|x_i^t,x_{i_c}^t\right)} \quad (10)$$

where x_{i_c} is the common cause of x_i obtained by Equation.7 and Equation.8. Equation.10 not only can accurately calculate the transfer entropy of x_{i_p} to x_i without the influence of common cause x_{i_c}, but also indicate the probability of causing x_i to generate an alarm if an alarm occurs in x_{i_p}. Like DTE and TE, ATE also needs to be tested for significance.

3.3 Active Dynamic Transfer Entropy

In the actual chemical process, the transfer of information between variables takes a certain amount of time. The proposed approach is also capable of extracting information related to propagation time in the structure. The active propagation time between variables by the following equations,

$$ATE_{x_{i_p}{}^t\to x_i>x_{i_p}{}^{t-h}\to x_i}=\sum_{x_i^{t+1},x_i^t,x_{i_p}{}^{t-h},x_{i_c}^t,x_{i_p}{}^t} p\left(x_i^{t+1},x_i^t,x_{i_p}{}^{t-h},x_{i_c}^t,x_{i_p}{}^t\right)\log_2\frac{p\left(x_i^{t+1}\middle|x_i^t,x_{i_p}{}^{t-h},x_{i_c}^t,x_{i_p}{}^t\right)}{p\left(x_i^{t+1}\middle|x_i^t,x_{i_p}{}^{t-h},x_{i_c}^t\right)} \quad (11)$$

$$ATE_{x_{i_p}{}^{t-h}\to x_i>x_{i_p}{}^t\to x_i}=\sum_{x_i^{t+1},x_i^t,x_{i_p}{}^{t-h},x_{i_c}^t,x_{i_p}{}^t} p\left(x_i^{t+1},x_i^t,x_{i_p}{}^t,x_{i_c}^t,x_{i_p}{}^{t-h}\right)\log_2\frac{p\left(x_i^{t+1}\middle|x_i^t,x_{i_p}{}^t,x_{i_c}^t,x_{i_p}{}^{t-h}\right)}{p\left(x_i^{t+1}\middle|x_i^t,x_{i_p}{}^t,x_{i_c}^t\right)} \quad (12)$$

$$\begin{aligned}ATE_{x_{i_p}{}^{t-h}\to x_i>x_{i_p}{}^t\to x_i}&=\sum_{x_i^{t+1},x_i^t,x_{i_p}{}^{t-h},x_{i_c}^t,x_{i_p}{}^t} p\left(x_i^{t+1},x_i^t,x_{i_p}{}^t,x_{i_c}^t,x_{i_p}{}^{t-h}\right)\log_2\frac{p\left(x_i^{t+1}\middle|x_i^t,x_{i_p}{}^t,x_{i_c}^t,x_{i_p}{}^{t-h}\right)}{p\left(x_i^{t+1}\middle|x_i^t,x_{i_p}{}^t,x_{i_c}^t\right)}\times\frac{p\left(x_i^{t+1}\middle|x_i^t,x_{i_p}{}^{t-h},x_{i_c}^t\right)}{p\left(x_i^{t+1}\middle|x_i^t,x_{i_p}{}^t,x_{i_c}^t,x_{i_p}{}^{t-h}\right)} \\ &=\sum_{x_i^{t+1},x_i^t,x_{i_p}{}^{t-h},x_{i_c}^t,x_{i_p}{}^{t-h}} p\left(x_i^{t+1},x_i^t,x_{i_p}{}^t,x_{i_c}^t,x_{i_p}{}^{t-h}\right)\log_2\frac{p\left(x_i^{t+1}\middle|x_i^t,x_{i_p}{}^{t-h},x_{i_c}^t\right)}{p\left(x_i^{t+1}\middle|x_i^t,x_{i_p}{}^t,x_{i_c}^t\right)}\end{aligned} \quad (13)$$

Equation.11 represents the amount of information that x_i flows from $x_{i_p}{}^t$ is more than that x_i is transmitted from $x_{i_p}{}^{t-h}$, and Equation.12 represents the amount of information that $x_{i_p}{}^t$ flows from $x_{i_p}{}^{t-h}$ is more than $x_{i_p}{}^{t-h}$ flows from $x_{i_p}{}^t$. Due to the detection asymmetry of the information entropy, we need to confirm that the prediction performance of $x_{i_p}{}^{t-h}$ to x_i is improved compared with the prediction performance of $x_{i_p}{}^t$ to x_i. We

subtract Equation.12 from Equation.11 to obtain the DTE value in Equation.13. If the DTE value is significant at the time h, it proves that $x_{i_p}^{t-h}$ is more suitable for predicting x_i. Since the chemical process is unstable and periodic , there may be multiple h corresponding DTE values are significant on the path x_{i_p} to x_i. Combine the results in Equation.13 with Equation.10, the ADTE for different propagation times is calculated as follow.

$$ADTE_{x_{i_p}^{t-h}\to x_i} = \sum_{x_i^{t+1},x_i^t,x_{i_c}^t,x_{i_p}^{t-h}} p\left(x_i^{t+1}, x_i^t, x_{i_c}^t, x_{i_p}^{t-h}\right)\log_2 \frac{p\left(x_i^{t+1}\middle| x_i^t, x_{i_c}^t, x_{i_p}^{t-h}\right)}{p\left(x_i^{t+1}\middle| x_i^t, x_{i_c}^t\right)} \quad (14)$$

This paper retains all ADTE values corresponding to DTE values that are significant, which is useful in the later structural search process.

3.4 Structure Searching

After obtaining the transfer entropy values for each propagation time, we propose a structure search method using the greedy search algorithm, and the score of each structure is given as follow:

$$Score_{ADTE}(G_{\text{greedy}}) = \sum_{ed=1}^{n} (ADTE_{ed} - \lambda_1 \log(h_{ed})) - \lambda_2 \log(n) \quad (15)$$

where $Score_{ADTE}(G_{\text{greedy}})$ represents the ADTE-based score of each structure searched by greedy algorithm. n represents the number of directed edges in the structure obtained by greedy search, and λ_1 and λ_2 are two penalty scale parameters, respectively. The penalty coefficients are used to limit the complexity of the structure and reduce the effect of the long propagation time caused by periodic data. $ADTE_{ed}$ and h_{ed} represent the ADTE value and the propagation time of the ed^{th} direction edge in each structure G_{greedy}. After scoring each structure, according to Equation.16, the highest-ranking structure is obtained as the final Bayesian network structure:

$$G_{\max} = \arg \max_{G_{greedy} \in G^{all}} score_{\mathrm{ADTE}}\left(G_{greedy}\right) \tag{16}$$

3.5 Structure Integration

After obtaining the Bayesian network structure of each sub-block, we add virtual variables to integrate different sub-blocks.

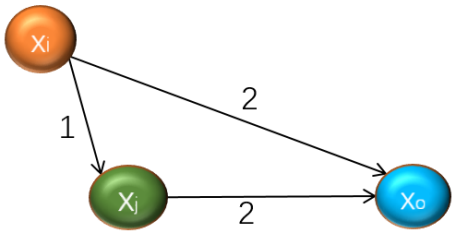

Fig.3 Variable relationship before structural integration

In Figure.3, it takes one sampling time for the alarm of x_i to effect x_j, and two sampling times for the alarm in x_j to effect x_o. In the parameter training process, the data x_i^t, x_j^{t+1}, and x_o^{t+3} should be included. However, it requires two sampling times from x_i to x_o, which is same as the time it takes for x_j to effect x_o. In this case, we use the concept of virtual variable to achieve structural integration, as shown in Figure.4.

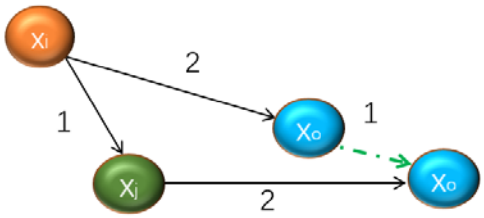

Fig.4 Variable relationship after structural integration

Adding the virtual variable significantly improves the accuracy of the alarm propagation structure. However, there is an additional computational cost incurred due to the increased number of variables.

3.6 Alarm Source Tracing Strategy

After establishing the structure and training the variable parameters, a simple alarm source

tracing strategy can be developed as shown in Equations.17 and Equations.18:

$$P_{\text{single},i} = \sum_{j=1}^{k} P_j / k \tag{17}$$

$$P_{multi} = \sum_{i=1}^{n_a} P_{\text{single},i} \tag{18}$$

Equation.17 represents a single alarm source tracing strategy, where k represents the number of all variables which the alarm path has passed through, and P_j represents the alarm probability of variable x_j in structure $G_{\max}$. $P_{\text{single},i}$ represents the score of alarm propagation path of alarm x_i. When multiple alarms occur simultaneously, according to Equation.18, the scores corresponding to each path of the alarm root variable are calculated. The alarm root variable is determined by the largest P_{multi} of the multi-alarm propagation path and n_a represents the number of alarm variables. The overall alarm root analysis step is shown in Figure.5.

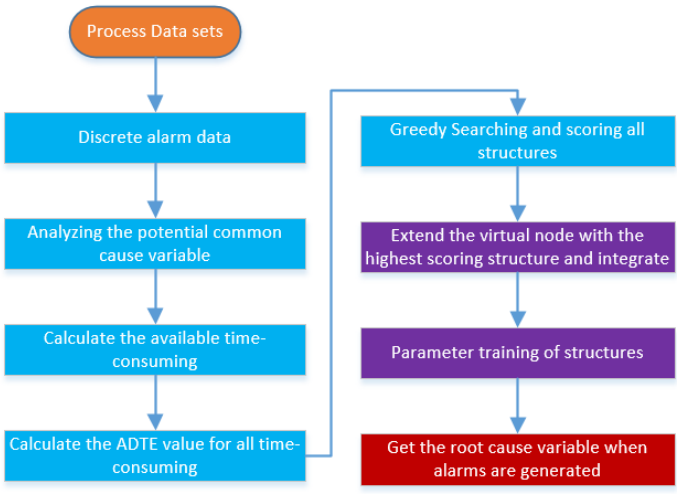

Fig.5 Alarm source tracing step of Bayesian network based on ADTE

4. SIMULATION

This section illustrates the importance of eliminating false causality during the construction of alarm structures based on Tennessee Eastman Problem (TEP)[35-38]. We use BIC, BDE, and

MBTE[31,33] methods to compare with and further demonstrate the superiority of the proposed method.

The TEP process consists of 41 measured variables XMEAS (1-41) and 12 control variables XMV (1-12) and the variable distribution and variable information are shown in Figure.6 and Table.1, respectively. In the experimental data set of TEP, there are 21 types of IDV (1-21) faults and each fault contains 960 samples. In this paper, the data set of IDV1 is used to verify the effectiveness of proposed method. IDV1 is a step fault and the root cause of this fault is FF4, which represents the change of the A/C feed ratio.

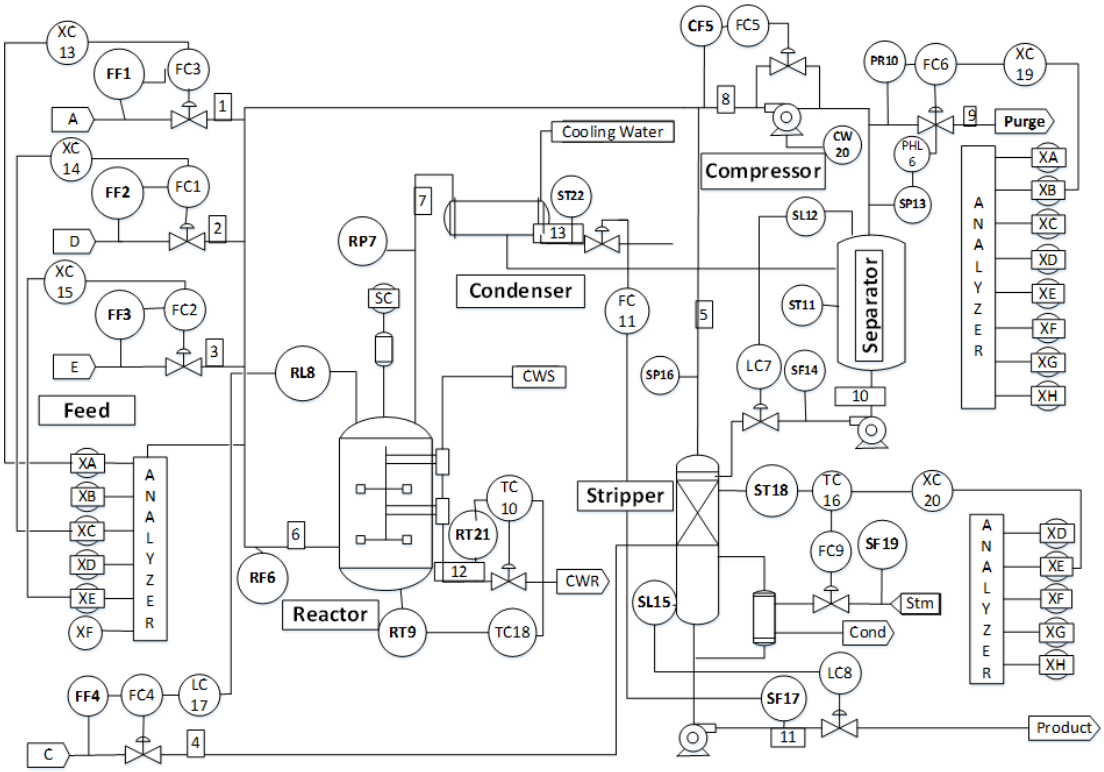

Fig.6 The process of Tennessee Eastman

Tab1. The description of 23 variables in TE process

Variable number	Variable symbol	Type	
FF1	XMEAS(1)	A feed (stream 1)	Feed
FF2	XMEAS(2)	D feed (stream 2)	
FF3	XMEAS(3)	E feed (stream 3)	
FF4	XMEAS(4)	Total feed (stream 4)	

CF5	XMEAS(5)	Recycle flow (stream 8)	Compressor
RF6	XMEAS(6)	Reactor feed rate (stream 6)	Reactor
RP7	XMEAS(7)	Reactor pressure	
RL8	XMEAS(8)	Reactor Level	
RT9	XMEAS(9)	Reactor temperature	
PR10	XMEAS(10)	Purge rate (Stream 9)	Purge
ST11	XMEAS(11)	Product set temp	Separator
SL12	XMEAS(12)	Product set level	
SP13	XMEAS(13)	Product set pressure	
SF14	XMEAS(14)	Product set underflow (stream 10)	
SL15	XMEAS(15)	Stripper level	Stripper
SP16	XMEAS(16)	Stripper pressure	
SF17	XMEAS(17)	Stripper underflow (stream 11)	
ST18	XMEAS(18)	Stripper temperature	
SF19	XMEAS(19)	Stripper steam flow	
CW20	XMEAS(20)	Compressor work	Compressor
RT21	XMEAS(21)	Reactor cooling water outlet temp	Reactor
ST22	XMEAS(22)	Separator cooling water outlet temp	Separator
CF23	XMV(11)	Condenser	Condenser

4.1 Causality Structure learning

In this section, causality structure learning will be divided into four parts: sub-blocks segmentation and variable selection, ADTE value calculation, optimal structure extraction and virtual variable expansion.

4.1.1 Sub-blocks Segmentation and Variable Selection

23 common variables in Table.1 are divided into three sub-blocks by the segmentation principle in section 2.3. The sub-blocks and the associated variables between adjacent sub-blocks are given in Table.2:

Tab2. The sub-blocks of TE process

Sub-block	Units	Variables
Sub1	feed、reactor、condenser, compressor, venting	FF1,FF2,FF3,FF4,RF6,RP7,RL8,RT9, RT21, ***CF23***,CF5,CW20
Sub2	Condenser, compressor, Venting, separator	***CF23***,CF5,CW20, PR10, ***ST11,SL12,SP13,SF14, ST22***

Sub3	Separator (part), stripper	***ST11,SL12,SP13,SF14,ST22,*** SL15,SP16,SF17,ST18,SF19

After dividing the TEP into three sub-blocks, we select alarm variables to establish the causality structure. Table.3 shows the alarm probability of each variable in normal case and IDV1 abnormal case.

Tab3. The alarm probability under normal condition and IDV1

Variable	Alarm probability under normal condition	Alarm probability under IDV（1）	Variable	Alarm probability under normal condition	Alarm probability under IDV（1）
FF1	1.63	92.09	SP13	1.4	31.51
FF2	0.93	2.56	SF14	0.23	1.28
FF3	4.53	28.95	SL15	0.58	0
FF4	0.35	89.07	SP16	1.16	26.74
CF5	0.47	0	SF17	0	0.12
RF6	0.23	4.19	ST18	5.81	84.77
RP7	1.05	31.51	SF19	6.4	75.35
RL8	0.7	23.26	CW20	3.26	33.49
RT9	0.7	1.28	RT21	0	23.26
PR10	0.47	30.07	ST22	1.05	19.53
ST11	0.93	27.56	CF23	0	0.23
SL12	0.7	0.35	/	/	/

In the data pre-processing step, variables which alarm probability do not change substantially are unrelated to IDV1 fault and will not be considered in this simulation. Through the information in Table.3, the sub-blocks of Table.2 can be simplified, as shown in Table.4. The later simulation in this paper is based on the sub-blocks division results in Table.4.

Tab4. The optimal sub-blocks of TE process

Sub-block	Variables
Sub1	FF1，FF2， FF3，FF4，RF6，RP7，RL8， RT21， CW20
Sub2	CW20， PR10， ST11， SP13，ST22
Sub3	ST11，SP13， ST22， SP16， ST18， SF19

4.1.2 ADTE

After obtaining the variables in each sub-block, we calculate the potential common cause

variables. To this end, the simulation results of Sub1 will be described in detail, and similar results were obtained using Sub2 and Sub3. Calculated by the method proposed in section 3.1, the results of the nine variables in Sub1 are shown in Figure.7.

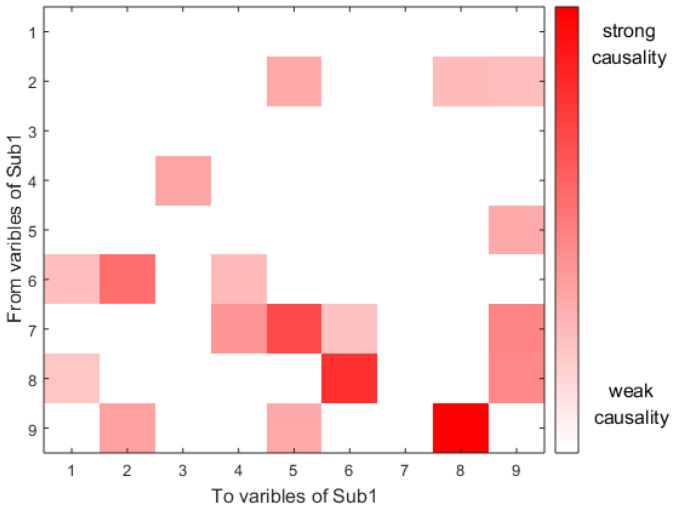

Fig.7 Potential common cause variables analysis

The transfer relationship between the variables can be seen from Figure.7. The white area represents that the value of the transfer entropy between the variables has not passed the significance test. The red area represents that there is a transfer relationship between the variables, and the deeper the color, the stronger the transfer relationship. Further, the potential common cause variables of each variable in sub1 are listed in Table.5.

Tab5. The potential common cause variables of each variable in sub1

Variable	The potential common cause variable
FF1	RP7,RT21
FF2	RP7,CW20
FF3	FF4
FF4	RP7,RL8
RF6	FF2,RL8,CW20
RP7	RL8,RT21
RL8	None
RT21	FF2,CW20
CW20	FF2,RF6,RL8,RT21

The information related to potential common cause variables is brought into ADTE for

calculation. Considering the computational complexity of TEP, the maximum alarm propagation time between variables is defined as ten samples. Figure.8 shows the relationship strength between variables according to the ADTE values at different propagation time, the maximum time lag is settled as 8 for calculation. In Figure.7, the white area represents that the value of the transfer entropy between the variables has not passed the significance test. The deeper color in Figure.8, the stronger causality.

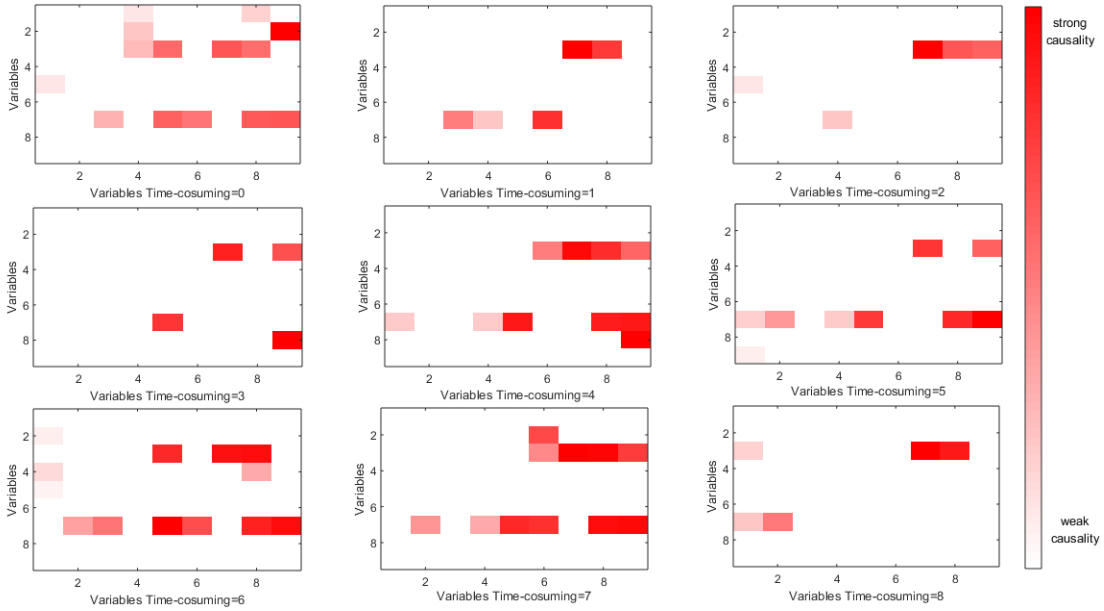

Fig.8 The ADTE values of Sub1 at different propagation time

It can be found that the same path between two variables may correspond to different propagation times, where RL8 to FF4 have five choices for propagation time, i.e. 2, 3, 5, 6 and 8. The reason for this phenomenon is the periodic characteristics of some variables or control loops in the chemical process. All this information should be preserved. Another advantage is that the ADTE can find relationships that were missed by previous studies. For example, the path from FF3 to CW20 does not exist in the initial data set, but there is a causal relationship when the propagation time is three, four, five, and six sample times. In the structure search step, the proposed method will automatically select the optimal

propagation time to build the Bayesian network structure based on Equation.16 and Equation.17. After obtaining the ADTE value between the variables, it will search the optimal structure through the method in section 3.4, in which the time penalty term λ_1=0.17 and the structural complexity penalty term λ_2=0.01. The result of traditional BIC, BDE, MBTE and ADTE are compared with Sub1 data, as shown in Figure.9-12.

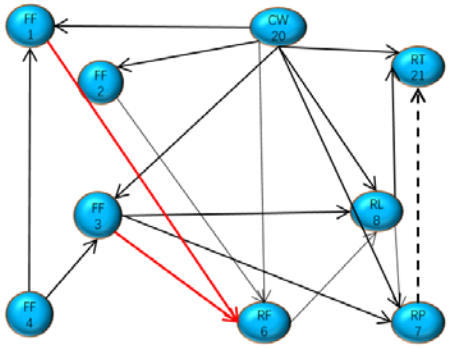

Fig.9 Sub1 Bayesian network structure based on BIC.

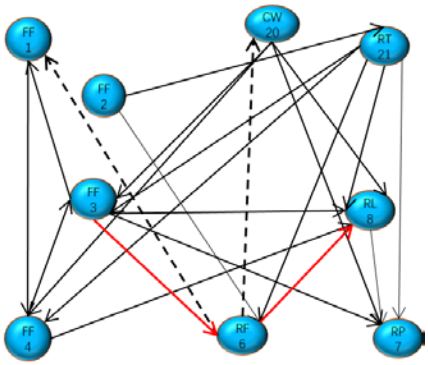

Fig.10 Sub1 Bayesian network structure based on BDE.

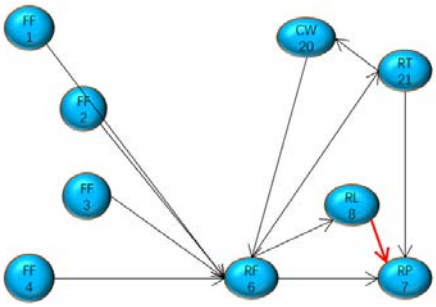

Fig.11 Sub1 Bayesian network structure based on MBTE.

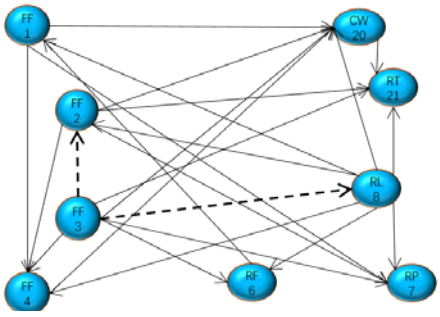

Fig.12 Sub1 Bayesian network structure based on ADTE.

The black line indicates that the relationship identified by data is consistent with the actual process, the dotted line indicates that the relationship identified from data is inconsistent with the actual process, and the red line indicates an important variable relationship that is not denied from the data. Compared to the structures obtained by BIC and BDE, MBTE and ADTE have significant advantages. However, the structure of MBTE is relatively simple. It may miss several relationships worthy of analysis, and it is difficult to distinguish between similarity and causality. For example, RF6, the feed rate for FF1, FF2, and FF3, varies synchronously with the reactor pressure RP7, and there only exists similarity between RF6 and RP7 rather than causal relationship. The causality relationship between RF6 and RP7 based on MBTE method is very strong, while ADTE can correctly find there is no causality relationship between them. Table.6 is a summary of the four methods to find the relationship between variables, where Y represents the correct result, O represents the opposite result and N represents lost important relationship result.

Tab6. Structure learning result of BDE, BIC, MBTE, and ADTE in sub1

Method	Y	O	N	Correct rate
BIC	15	1	2	83.3%
BDE	18	2	2	81.8%
MBTE	10	1	0	90.9%
ADTE	22	2	0	91.7%

The ADTE-based Bayesian network method has the best performance and can mine deeper

relationships. Table.7 is the adjacency matrix after the integration of three sub-blocks, where the number represents propagation time in optimal structure.

Tab7. Data driven Bayesian network structure preliminary fusion results of TE process

	FF 1	FF 2	FF 3	FF 4	RF 6	RP 7	RL 8	CW 20	RT 21	PR 10	ST 11	SP 13	ST 22	SP 16
FF1	0	0	0	1	0	1	0	1	0	0	0	0	0	0
FF2	0	0	0	1	0	4	0	6	1	0	0	0	0	0
FF3	0	7	0	1	1	5	1	1	4	0	0	0	0	0
FF4	0	0	0	0	0	0	0	1	0	0	0	0	0	0
RF6	1	0	0	0	0	0	0	0	0	0	0	0	0	0
RP7	0	0	0	0	0	0	0	0	0	0	0	0	0	0
RL8	2	6	0	3	1	1	0	1	1	0	0	0	0	0
CW20	0	0	0	0	0	0	0	0	4	0	1	0	1	0
RT21	0	0	0	0	0	0	0	0	0	0	0	0	0	0
PR10	0	0	0	0	0	0	0	0	0	0	0	0	0	0
ST11	0	0	0	0	0	0	0	0	0	0	0	0	0	0
SP13	0	0	0	0	0	0	0	0	0	0	0	0	0	1
ST22	0	0	0	0	0	0	0	0	0	4	1	1	0	0
SP16	0	0	0	0	0	0	0	0	0	0	0	0	0	0

The propagation time of path FF3 to FF2 is 7 sample times, which is not consistent with the common sense. The correct case is that the propagation time of path FF2 to FF3 should be zero. The reason is that, FF2 has less impact on IDV1 fault, while FF3 affects RL8 (reactor grade) and control loop causes FF2 to generate alarms. From Tab.7, we can find that propagation time of the path FF3 to RL8 is 1 sample time and path RL8 to FF2 is 6 sample times, which forms a closed loop among FF2, FF3, RL8. This phenomenon also proves that the method proposed in this paper can deeply explore the dynamic propagation relationship between variables. Based on the adjacency matrix, the alarm propagation structure of TEP is shown in Figure.13.

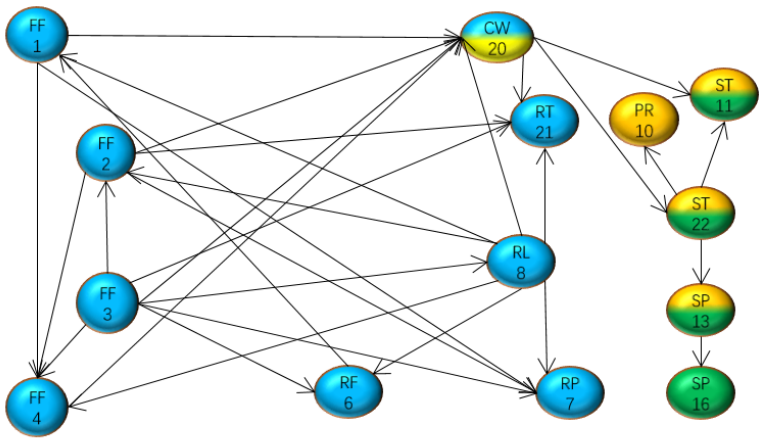

Fig.13 Bayesian network structure based on ADTE

Blue, yellow and green colors represent the variables of the first sub-block, the second sub-block and the third sub-block respectively. Blue-yellow represents the associated variables of the first sub-block and the second sub-block. Yellow-green represents the associated variables of the second sub-block and the third sub-block. In the parameter training, this work will explore the root alarm of IDV1 alarm according to Figure.13.

4.2 Alarm Source Tracing Analysis

As the propagation time between variables in Table.7 is different, after getting the alarm propagation structure in Figure.13, it is necessary to perform virtual variable expansion according to the method proposed in section 3.5, and the virtual variable should be regarded as an independent variable for parameter training. The result of the expansion is shown in Figure.14.

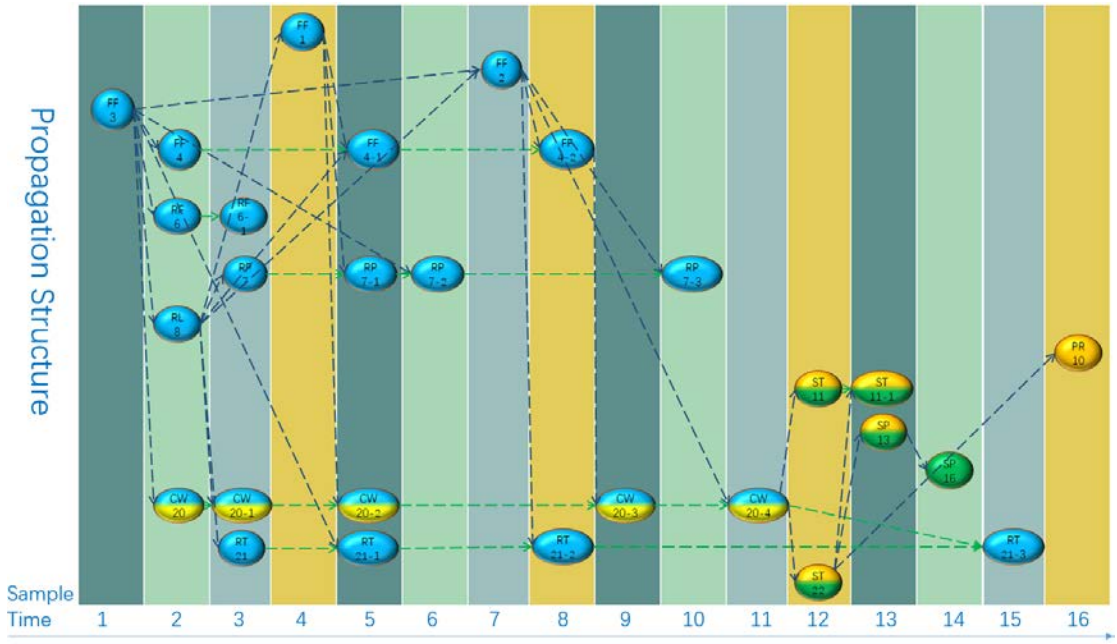

Fig.14 The expansion structure based on ADTE

The blue dotted line represents the propagation path between variables, the green dotted line represents the extended propagation path.

4.2.1 Single Alarm Source Tracing Analysis

The 28 variables (including the virtual variables) in Figure.14 are trained through the TEP data set. Assume that one alarm occurs in SP13 and substitute SP13=1 as evidence into the Bayesian network structure, the alarm probability of each variable is shown in Table.8.

Tab.8. Alarm probability for each variable when SP13 alarm

Variable	FF3	FF4	RF6	RL8	CW20	RF6-1	RP7
Normal	0.6911	0.0928	0.9569	0.7495	0.6024	0.9647	0.6674
Alarm	0.3089	0.9072	0.0431	0.2505	0.3976	0.0353	0.3326
Variable	CW20-1	RT21	FF1	FF4-1	RP7-1	CW20-2	RT21-1
Normal	0.5921	0.7564	0.7153	0.0913	0.6665	0.5789	0.7558
Alarm	0.4079	0.2436	0.2847	0.9087	0.3335	0.4211	0.2442
Variable	RP7-2	FF2	FF4-2	RT21-2	CW20-3	RP7-3	CW20-4
Normal	0.6662	0.9890	0.0875	0.7610	0.5617	0.6696	0.5421
Alarm	0.3338	0.0110	0.9125	0.2390	0.4383	0.3304	0.4579
Variable	ST11	ST22	ST11-1	SP13	SP16	RT21-3	PR10
Normal	0.6619	0.5870	0.6608	0.0000	0.1919	0.7557	0.6236
Alarm	0.3381	0.4130	0.3392	1.0000	0.8081	0.2443	0.3764

According to Table.8, when SP13 alarms, the alarm probability of each variable can be obtained. The propagation path and score corresponding to each alarm roots are shown in Appendix. A.

As seen from Appendix. A, path 7 has the highest score and should be defined as the alarm propagation path. Through the method proposed in this paper, FF4 is detected as the root alarm variable, which is in line with the actual situation and has practical significance. The red line represents the identified propagation path in Figure.15

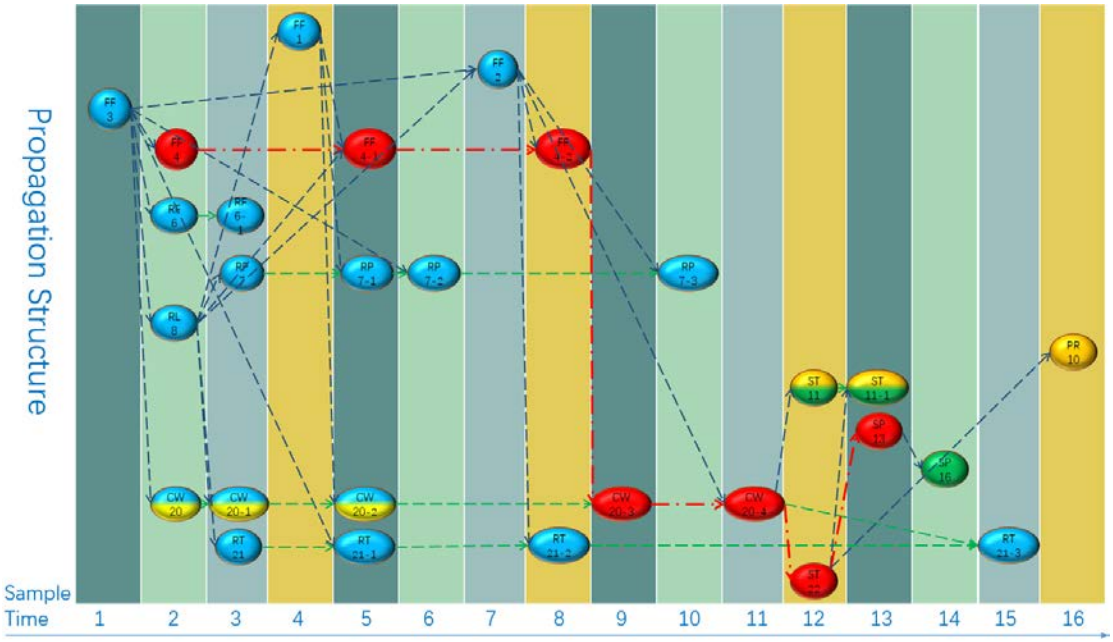

Fig.15 Propagation path for the alarming of SP13 based on ADTE

As can be seen from Figure.15, when SP13 alarms, FF4 is the source of the alarm flood, and the time FF4 generating an abnormality is about 14 sample times before the SP13 alarms. At the same time, there is 80% chance of alarming for SP16 at the next sample time. This information will help the operator to handle the abnormal situation.

4.2.2 Multiple Alarms Source Tracing Analysis

Like the analysis in 4.2.1, in multiple alarm source tracing, we assume that RT21-3, ST22 and SP16 simultaneously alarm. RT21-3=1, ST22=1 and SP16=1 are substituted into the Bayesian

network structure as evidence, and the alarm probability of each variable is shown in Table.9.

Tab.9. Alarm probability for each variable when RT21-3, ST22 and SP16 simultaneously alarm

Variable	FF3	FF4	RF6	RL8	CW20	RF6-1	RP7
Normal	0.5999	0.0923	0.9551	0.6736	0.3630	0.9596	0.6302
Alarm	0.4001	0.9077	0.0449	0.3264	0.6370	0.0404	0.3698
Variable	CW20-1	RT21	FF1	FF4-1	RP7-1	CW20-2	RT21-1
Normal	0.3305	0.6539	0.6885	0.0916	0.6322	0.2894	0.6318
Alarm	0.6695	0.3461	0.3115	0.9084	0.3678	0.7106	0.3682
Variable	RP7-2	FF2	FF4-2	RT21-2	CW20-3	RP7-3	CW20-4
Normal	0.6328	0.9833	0.0894	0.5887	0.1850	0.6470	0.0778
Alarm	0.3672	0.0167	0.9106	0.4113	0.8150	0.3530	0.9222
Variable	ST11	ST22	ST11-1	SP13	SP16	RT21-3	PR10
Normal	0.4324	0.0000	0.4352	0.0121	0.0000	0.0000	0.4524
Alarm	0.5676	1.0000	0.5648	0.9879	1.0000	1.0000	0.5476

According to Table.9, when RT21-3, ST22 and SP16 simultaneously alarm, the alarm probability of each variable can be obtained. The propagation path and score corresponding to each alarm root are shown in Appendix. B.

As seen from Appendix. B, path 7 is the alarm propagation path because of the highest score. In the case where multiple alarms occur at the same time, FF4 is still detected as the root alarm variable, which is in line with the fact. The propagation path is indicated by the red dot line in Figure 16.

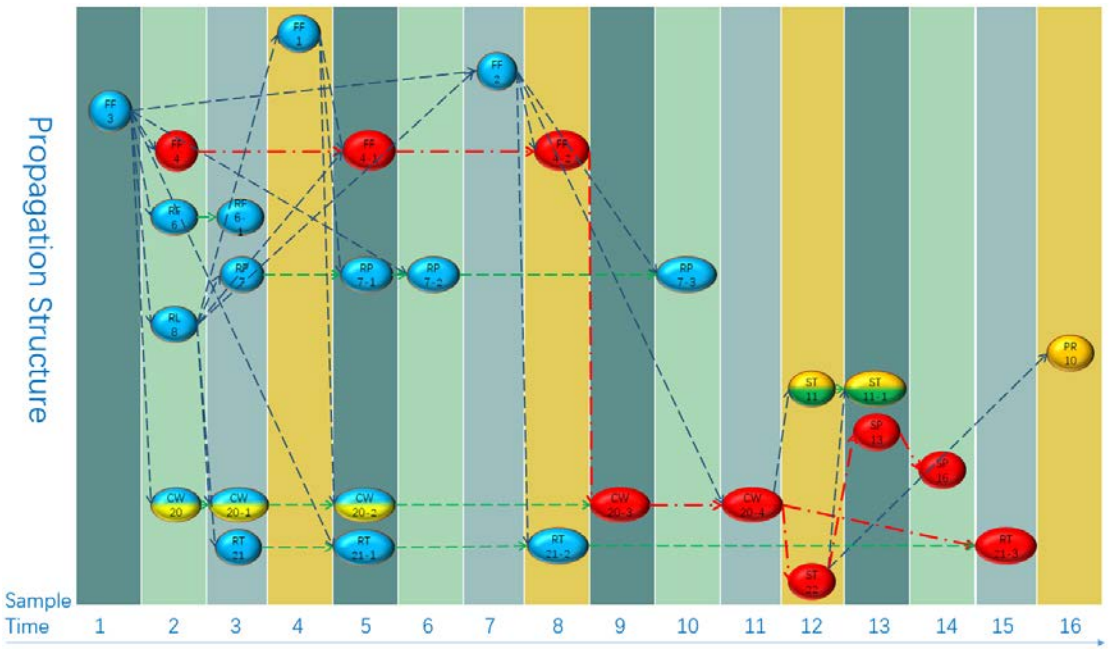

Fig.16 Propagation path for the alarming of SP16, ST22, PR10 based on ADTE

According to the simulation results of 4.2.1 and 4.2.2, the ADTE-based Bayesian network proposed in this paper can accurately analyze the alarm source under the alarm flood and assist the operator to handle the alarm quickly. In addition, when ST22, SP16 and RT21 alarms, according to Table.10, we can predict that PR10 has 54% chance of raising an alarm at the next sample time. It is easy to find that the ADTE-based Bayesian network can discover deeper transmission relationships, which is vital for solving the alarm flooding problems.

5. CONCLUSIONS

An ADTE-based Bayesian network method is proposed in this paper. The proposed method can accurately trace the alarm source. It is a complete alarm traceability analysis system and can help operators to respond to alarm flooding conditions quickly and accurately. Compared with the traditional alarm source tracing analysis methods, our method can distinguish the correlation and causality, and effectively solve the false causality problem caused by strong correlation between variables. Furthermore, this work establishes an alarm

active propagation structure based on the causal relationship between variables, which has great significance to the alarm system of the actual chemical process. In order to prove the effectiveness of the proposed method, some algorithms, such as BIC, BDE and MBTE, are used as comparative studies in the same benchmark, TEP. The simulation results demonstrate the superiority of the proposed method.

ACKNOWLEDGEMENT

This research is supported by the National Natural Science Foundation of China under Grant Nos. 61973022, 61573051 and 61473026.

REFERENCE

[1] Wang, J.; He, Y.L.; Zhu, Q.X. Energy and production efficiency optimization of an ethylene plant considering process operation and structure. *Industrial & Engineering Chemistry Research*. **2020**, 59, 1202-1217.

[2] Boyer S A. *SCADA: supervisory control and data acquisition*; International Society of Automation, **2009**.

[3] He, Y.L.; Tian, Y.; Xu, Y.; Zhu, Q.X.; Novel soft sensor development using echo state network integrated with singular value decomposition: Application to complex chemical processes. *Chemometrics and Intelligent Laboratory Systems*, **2020**, 200, 103981.

[4] Hu, W.; Chen, T.; & Shah, S. L. Detection of frequent alarm patterns in industrial alarm floods using itemset mining methods, *IEEE Transactions of Industrial Electronics*. **2018**, 65, 7290-7300.

[5] Kondaveeti S R.; Izadi I.; Shah S L.; Black, T. Graphical representation of industrial alarm

data. *IFAC Proceedings Volumes*. **2010**, 43, 181-186.

[6] Hu, W.; Shah, S. L.; & Chen, T. Framework for a smart data analytics platform towards process monitoring and alarm management, *Computers & Chemical Engineering*. **2018**, 114, 225-244.

[7] Lai S.; Yang F.; Chen T.; Cao L. Accelerated multiple alarm flood sequence alignment for abnormality pattern mining. *Journal of Process Control*. **2019**, 82, 44-57.

[8] Fu F.; Wang D.; Li L.; Wu Z. Data-driven method for the quantitative fault diagnosability analysis of dynamic systems. *IET Control Theory & Applications*. **2019**, 13, 1197-1203.

[9] Cheng Y.; Izadi I.; Chen T. Pattern matching of alarm flood sequences by a modified Smith–Waterman algorithm. *Chemical engineering research and design*. **2013**, 91, 1085-1094.

[10] Chang C.; Yu C. On-line fault diagnosis using the signed directed graph. *Industrial & Engineering Chemistry Research*. **1990**, 29, 1290-1299.

[11] Fu F.; Wang D.; Liu P.; Li W. Evaluation of fault diagnosability for networked control systems subject to missing measurements. *Journal of the Franklin Institute*. **2018**, 355, 8766-8779.

[12] Briand L C.; Brasili V R.; Hetmanski C J. Developing interpretable models with optimized set reduction for identifying high-risk software components. *IEEE Transactions on Software Engineering*. **1993**, 19, 1028-1044.

[13] Guha R. On the interpretation and interpretability of quantitative structure–activity relationship models. *Journal of computer-aided molecular design*. **2008**, 22, 857-871.

[14] Jensen F V. *An introduction to Bayesian networks*; London: UCL press, **1996**.

[15] Nielsen T D.; Jensen F V. *Bayesian networks and decision graphs*; Springer Science &

Business Media, **2009**.

[16] Friedman N.; Linial M.; Nachman I.; Pe'er D. Using Bayesian networks to analyze expression data. *Journal of computational biology*. **2000**, 7, 601-620.

[17] Heckerman D.; Geiger D.; Chickering D M. Learning Bayesian networks: The combination of knowledge and statistical data. *Machine learning*. **1995**, 20, 197-243.

[18] Heo U.; Tan A C. Democracy and economic growth: A causal analysis. *Comparative Politics*. **2001**, 33, 463-473.

[19] Brovelli A.; Ding M.; Ledberg A.; Chen Y.; Nakamura R.; Bressler S L. Beta oscillations in a large-scale sensorimotor cortical network: directional influences revealed by Granger causality. *Proceedings of the National Academy of Sciences*. **2004**, 101, 9849-9854.

[20] Barnett L.; Barrett A B.; Seth A K. Granger causality and transfer entropy are equivalent for Gaussian variables. *Physical review letters*. **2009**, 103, 238701.

[21] Yu W.; Yang F. Detection of causality between process variables based on industrial alarm data using transfer entropy. *Entropy*. **2015**, 17, 5868-5887.

[22] Hu W.; Wang J.; Chen T.; Shah SL. Cause-effect analysis of industrial alarm variables using transfer entropies. *Control Engineering Practice*. **2017**, 64, pp 205-214.

[23] Lindner B.; Auret L.; Bauer M.; Groenewald JWD. Comparative analysis of Granger causality and transfer entropy to present a decision flow for the application of oscillation diagnosis. *Journal of Process Control*. **2019**, 79, 72-84.

[24] Hu W.; Chen T.; Shah S.L.; Hollender M. Cause and effect analysis for decision support in alarm floods. *IFAC World Congress*. **2017**, pp, 14505-14510.

[25] Zhu Q.; Meng Q.; Wang P.; He Y. Novel causal network modeling method integrating process

knowledge with modified transfer entropy: a case study of complex chemical processes. *Industrial & Engineering Chemistry Research*. **2017**, 56, 14282-14289.

[26] Wang Y.; Liu Y.; Khan F.; Imtiaz S. Semiparametric PCA and bayesian network based process fault diagnosis technique. *The Canadian Journal of Chemical Engineering*. **2017**, 95, 1800-1816.

[27] Gharahbagheri H.; Imtiaz S A.; Khan F. Root cause diagnosis of process fault using KPCA and Bayesian network. *Industrial & Engineering Chemistry Research*. **2017**, 56, 2054-2070.

[28] Tao D.; Sun J.; Wu X.; Li X.; Shen J.; Maybank SJ. Probabilistic tensor analysis with akaike and bayesian information criteria. *International Conference on Neural Information Processing*. **2007**, 791-801.

[29] Meloni A.; Ripoli A.; Positano V.; Landini L. Mutual information preconditioning improves structure learning of Bayesian networks from medical databases. *IEEE Transactions on Information Technology in Biomedicine*. **2009**, 13, 984-989.

[30] Antoniak C E. Mixtures of Dirichlet processes with applications to Bayesian nonparametric problems. *The annals of statistics*. **1974**, 1152-1174.

[31] Meng Q.; Zhu X.; Gao H.; He Y.; Xu Y. A novel scoring function based on family transfer entropy for Bayesian networks learning and its application to industrial alarm systems. *Journal of Process Control*. **2019**, 76, 122-132.

[32] Duan P.; Yang F.; Chen T.; Sirish L Shah. Direct causality detection via the transfer entropy approach. *IEEE transactions on control systems technology*. **2013**, 21, 2052-2066.

[33] Duan P.; Yang F.; Sirish L Shah.; Chen T. Transfer zero-entropy and its application for capturing cause and effect relationship between variables. *IEEE Transactions on Control Systems Technology*. **2015**, 23, 855–867.

[34] Zhu Q.; Luo Y.; He Y. Novel Multiblock Transfer Entropy Based Bayesian Network and Its Application to Root Cause Analysis. *Industrial & Engineering Chemistry Research*. **2019**, 58, 4936-4945.

[35] Yin, S.; Ding S.X.; Haghani A.; Hao H.; Zhang P. A comparison study of basic data-driven fault diagnosis and process monitoring methods on the benchmark Tennessee Eastman process. *Journal of process control*. **2012**, 22, 1567-1581.

[36] Xu Y.; Fan C.; Zhu Q.; Rajabifard A.; Chen N.; Chen Y.; He, Y. Novel Pattern-Matching Integrated KCVA with Adaptive Rank-Order Morphological Filter and Its Application to Fault Diagnosis. *Industrial & Engineering Chemistry Research*. **2020**, 59, 1619-1630.

[37] He Y.L.; Zhao Y.; Hu X.; Yan X.N.; Zhu Q.X.; Xu Y. Fault diagnosis using novel AdaBoost based discriminant locality preserving projection with resamples. Engineering Applications of Artificial Intelligence. **2020**, 103631.

[38] Kulkarni A.; Jayaraman V.K.; Kulkarni B.D. Knowledge incorporated support vector machines to detect faults in Tennessee Eastman Process. *Computers & chemical engineering*. **2005**, 29, 2128-2133.

TOC

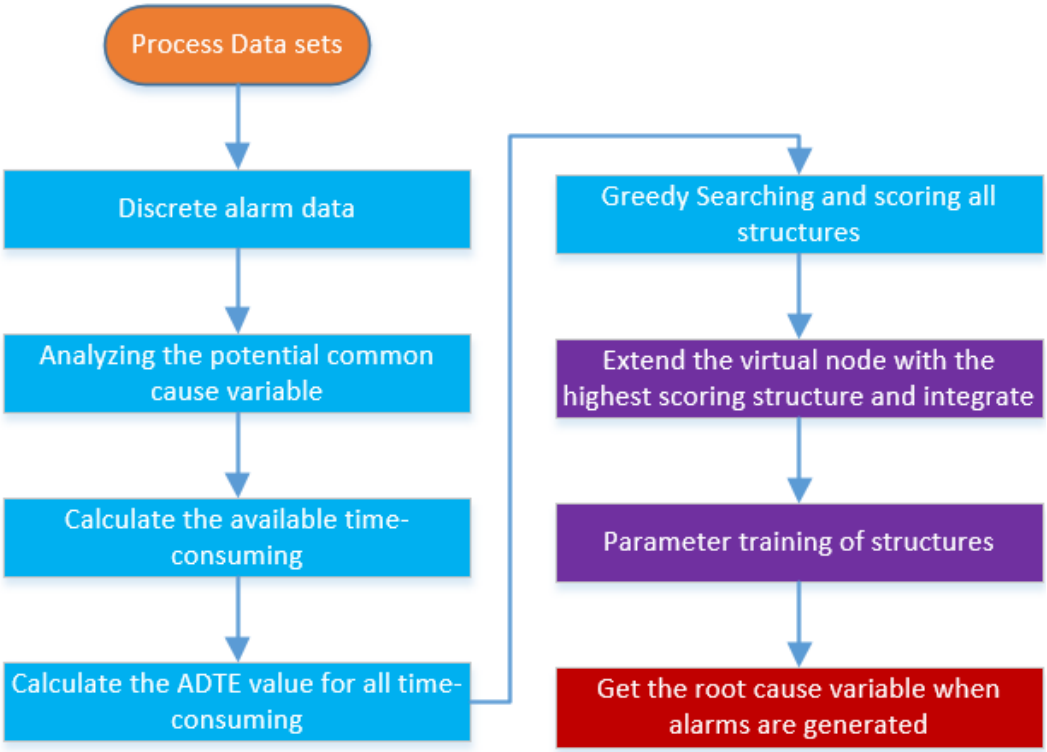
Process Data sets
Discrete alarm data
Analyzing the potential common cause variable
Calculate the available time-consuming
Calculate the ADTE value for all time-consuming
Greedy Searching and scoring all structures
Extend the virtual node with the highest scoring structure and integrate
Parameter training of structures
Get the root cause variable when alarms are generated